Proceedings of ICBioMed 2025 Symposium: AI for Healthcare: Advanced Medical Data Analytics and Smart Rehabilitation
DOI: 10.54254/2753-8818/2025.AU30835

Computational Modeling of Dynamic Supramammillary-Enhanced Adult Neurogenesis and Microglial Phagocytosis in Alzheimer's Disease

Guancheng Zhang

University of California San Diego, La Jolla, USA
guz006@ucsd.edu

Abstract. The supramammillary nucleus (SuM) regulates adult hippocampal neurogenesis (AHN), with potential implications for Alzheimer's disease (AD). Recent work suggests that SuM-enhanced adult-born neurons (ABNs) could influence microglial phagocytosis of amyloid-β (Aβ) plaques via TREM2-dependent pathways. Here, we applied an in-silico framework using publicly available single-cell transcriptomics to explore this hypothesis. Unlike simple linear models, we simulated dynamic and heterogeneous ABN activation, applying variable shifts in ABN module expression across individual cells. Stepwise analyses include Pearson and Spearman correlations and mutual information estimation. Results demonstrate that homogeneous linear activation fails to produce meaningful correlations, whereas heterogeneous stimulation reveals modest variability but no consistent strong association. These findings highlight the importance of biological heterogeneity and dynamic signaling in ABN–microglia interactions, suggesting that ABN maturation alone is insufficient to drive microglial plaque clearance. The framework provides a computational blueprint for hypothesis testing and informs the design of targeted wet-lab experiments.

Keywords: supramammillary nucleus (SuM), adult hippocampal neurogenesis (AHN), computational framework

1. Introduction

Alzheimer's disease (AD) is characterized by amyloid-β (Aβ) plaque accumulation, microglial dysfunction, and progressive neurodegeneration. Microglia, particularly TREM2+ subsets, can clear plaques but often show impaired phagocytic function in AD [1]. Parallel studies indicate that adult-born neurons (ABNs) in the dentate gyrus modulate local microglial states, linking neural plasticity to immune regulation [2].

The supramammillary nucleus (SuM) provides excitatory input to the dentate gyrus and can enhance ABN maturation. In vivo, Li and colleagues showed that optogenetic SuM stimulation increases ABN integration and promotes microglial phagocytosis of Aβ plaques in 5xFAD mice [3]. However, experimental verification requires sophisticated infrastructure.

This study translates the SuM–ABN–microglia hypothesis into a computationally tractable framework. Using publicly available single-cell datasets, we aim to test the dynamic and

DOI: 10.54254/2753-8818/2025.AU30835

heterogeneous effect of ABN activation on microglial phagocytosis. Emphasis is placed on stepwise hypothesis refinement and the importance of heterogeneity in neuroimmune interactions.

2. Background

Computational modeling of neuroimmune interactions in Alzheimer's disease (AD) requires methods that can capture both simple and complex patterns of association between cellular states. In this study, we integrate several statistical and machine-learning approaches—Pearson correlation, Spearman correlation, mutual information estimation, and LOESS smoothing—within a single-cell transcriptomic framework. Each of these methods plays a distinct role in testing the hypothesis that supramammillary (SuM)-enhanced adult-born neurons (ABNs) can modulate microglial phagocytosis through TREM2-dependent mechanisms.

Pearson correlation provides a classical measure of linear association between ABN module scores and microglial phagocytosis scores [4]. It is most sensitive to direct, proportional changes across the two variables, which makes it a natural first step in testing whether simulated SuM activation produces straightforward linear coupling between neuronal and microglial states. However, biological systems rarely behave in purely linear ways. For this reason, Spearman correlation, a rank-based measure, is also included [5]. Unlike Pearson, Spearman correlation can capture monotonic but non-linear relationships and is more robust to outliers and skewed distributions often present in single-cell transcriptomics [6].

Beyond correlation, we employ mutual information (MI), a measure derived from information theory that quantifies the reduction in uncertainty about one variable given knowledge of another [7]. MI has the advantage of detecting non-linear, non-monotonic dependencies, which are common in biological systems where feedback loops, thresholding, and stochasticity obscure simple relationships. MI has been increasingly adopted in single-cell analysis and systems biology for uncovering hidden dependencies between gene expression and functional modules [8,9]. Applying MI in parallel with Pearson and Spearman enables us to identify whether subtle or higher-order dependencies exist between ABN activity and microglial function, even when correlations appear weak.

Finally, we use LOESS (locally estimated scatterplot smoothing), a non-parametric regression tool for visualization [10]. LOESS does not assume any specific functional form between variables; instead, it fits local regressions across subsets of data, providing a smoothed curve that highlights potential non-linear trends. In the context of our analysis, LOESS is applied to scatterplots of ABN module scores versus microglial phagocytosis scores, both before and after simulated SuM activation. This allows intuitive visual inspection of patterns that may not be captured by correlation or MI values alone [11,12].

Together, these methods create a layered analytic pipeline. We begin with linear correlation (Pearson), expand to monotonic trends (Spearman), extend to general dependence (MI), and finally visualize with non-parametric smoothing (LOESS). By applying these approaches to both homogeneous and heterogeneous simulations of ABN activation, we can systematically assess whether ABN variability has any measurable or hidden influence on microglial phagocytosis. The integration of these methods ensures that both simple and complex forms of association are evaluated, providing a balanced and interpretable computational framework for exploring SuM–ABN–microglia interactions in Alzheimer's disease.

DOI: 10.54254/2753-8818/2025.AU30835

3. Methods

Single-cell transcriptomic data from the mouse hippocampus were obtained from GSE140511, including wild-type (WT), TREM2 knockout (TREM2 KO), and WT 5xFAD groups [13]. Gene annotations were retrieved from Ensembl version 107 [14]. Raw count matrices were processed using Scanpy in Python. Cells expressing fewer than 200 genes or genes expressed in fewer than three cells were removed. Counts were normalized to 10,000 per cell and log-transformed. Highly variable genes (n=2,000) were selected for downstream analyses, and gene identifiers were mapped from Ensembl IDs to gene symbols.

ABNs were identified based on expression of DCX, PROX1, and CALB2, while microglia were defined using P2RY12 and CX3CR1 expression. TREM2-positive subsets were further delineated using TREM2 expression. Cells were flagged as positive if they expressed any corresponding marker genes. Gene set scores were computed for each cell, including an ABN module (NEUROD1, EOMES, SYN1) and a microglial phagocytosis module (TREM2, TYROBP, APOE, LPL).

Virtual SuM activation was simulated in a stepwise manner. First, a homogeneous +1 SD shift was applied across all ABN-positive cells. Pearson and Spearman correlations, along with mutual information, were calculated to assess the association between ABN scores and microglial phagocytosis scores. Stronger homogeneous shifts (0 to +5 SD) were subsequently applied to evaluate dose-dependent effects. Non-linear trends were visualized using LOESS smoothing. Heterogeneous activation was simulated by applying normally distributed random shifts proportional to the SD of ABN scores to individual ABNs, reflecting more biologically realistic variability. All correlations were recalculated for each simulation scenario.

4. Results

Under baseline conditions, ABN-positive cells exhibited minimal correlation with microglial phagocytosis. Pearson correlation was 0.030 ($p = 0.6133$), Spearman correlation was 0.015 ($p=0.8081$), and mutual information was 0.182 (Figure 1, Table 1). Homogeneous +2 SD simulation modestly increased ABN scores but did not meaningfully change correlations (Pearson 0.0303; Spearman 0.0146, $p=0.8081$; MI 0.0256), as visualized in scatterplots (Figure 2).

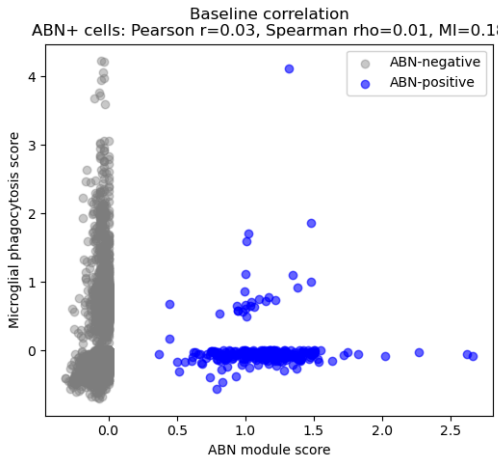

Figure 1. Baseline correlation between ABN module scores and microglial phagocytosis

Baseline correlation between ABN module scores and microglial phagocytosis scores in ABN-positive cells. Scatterplot shows ABN-positive cells (blue) and ABN-negative cells (gray). Pearson

DOI: 10.54254/2753-8818/2025.AU30835

and Spearman correlations, as well as mutual information, are reported for the unperturbed dataset. ABN-negative cells show low phagocytosis scores, consistent with expected baseline microglial activity.

Table 1. Baseline correlation metrics (ABN-positive cells, no simulation)

Metric	Value
Pearson correlation	0.0303
Spearman correlation	0.0146
Mutual Information	0.0182

Baseline correlation metrics between ABN module scores and microglial phagocytosis. Pearson, Spearman, and mutual information values are calculated for ABN-positive cells without any simulated SuM activation.

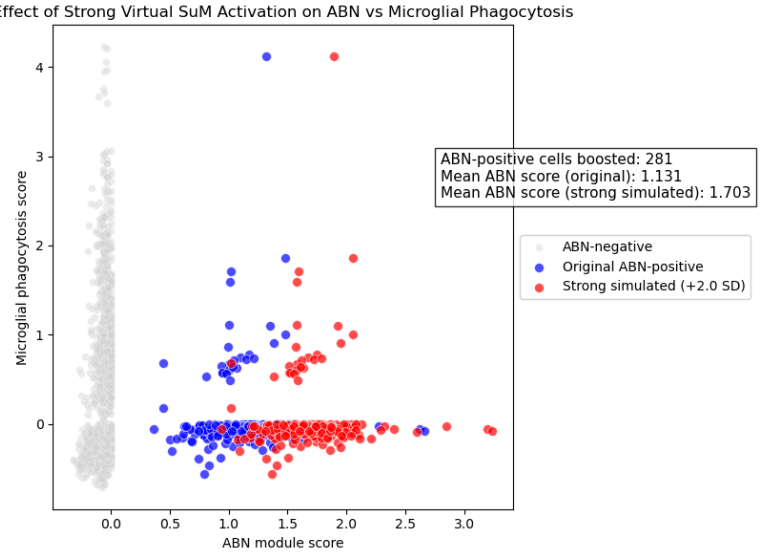

Figure 2. Effect of homogeneous +2 SD virtual SuM activation on ABN-positive cells

Effect of homogeneous +2 SD virtual SuM activation on ABN-positive cells. Scatterplots compare original ABN module scores (blue) with simulated scores after uniform +2 SD increase (red) against microglial phagocytosis. ABN-negative cells are shown in gray. Summary annotations indicate the number of ABN-positive cells and mean module scores before and after simulation. No significant correlation increase is observed.

Progressively stronger homogeneous shifts (0 to +5 SD) yielded little or no fluctuations in Pearson and Spearman correlations and no changes in mutual information, indicating that uniform activation alone is insufficient to predict microglial responses (Figure 3, Table 2). LOESS smoothing suggested no emergent non-linear trends between ABN scores and microglial phagocytosis.

DOI: 10.54254/2753-8818/2025.AU30835

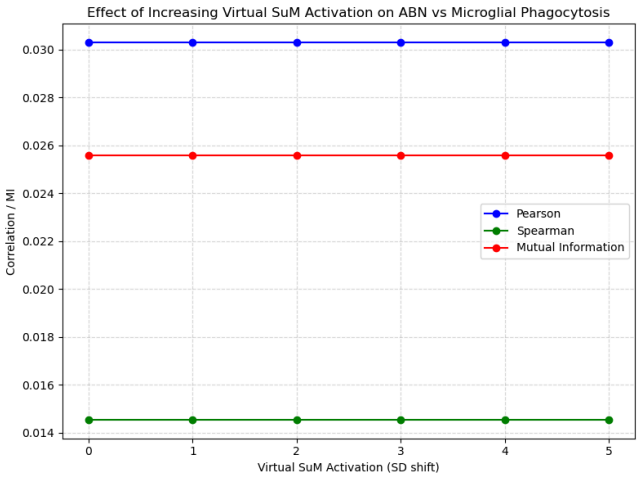

Figure 3. Stepwise homogeneous SuM activation and correlation metrics

Stepwise homogeneous SuM activation (0 to +5 SD) and correlation metrics. Line plots display Pearson (blue), Spearman (green), and mutual information (red) between ABN and microglial scores for each level of homogeneous activation. Minimal changes in correlations indicate that uniform increases in ABN activity are insufficient to drive strong microglial responses.

Table 2. Correlation metrics under homogeneous SuM activation (SD shift: 0 to +5)

SD shift	Pearson	Spearman	Mutual Information
0	0.0303	0.0146	0.0256
1	0.0303	0.0146	0.0256
2	0.0303	0.0146	0.0256
3	0.0303	0.0146	0.0256
4	0.0303	0.0146	0.0256
5	0.0303	0.0146	0.0256

Correlation metrics for progressively stronger homogeneous SuM activation (0 to +5 SD). Values of Pearson correlation, Spearman correlation, and mutual information are shown for each SD shift applied uniformly across ABN-positive cells.

Heterogeneous stimulation, in which individual ABNs received normally distributed perturbations, produced slightly more variable outcomes. Under a +2 SD heterogeneous simulation, Pearson correlation was 0.0034, Spearman correlation -0.0126 ($p=0.8341$), and mutual information was 0.0243 (Figure 4). Iterative heterogeneous simulations across SD shifts of 0–5 demonstrated modest fluctuations in correlation metrics, with Pearson correlations ranging from 0.0034 to 0.0526, Spearman correlations from -0.0126 to 0.0602, and mutual information from 0.0000 to 0.0698 (Figure 5, Table 3). Scatterplots confirmed that heterogeneous ABN perturbations increased variability in ABN module scores without inducing strong or consistent microglial phagocytic responses.

DOI: 10.54254/2753-8818/2025.AU30835

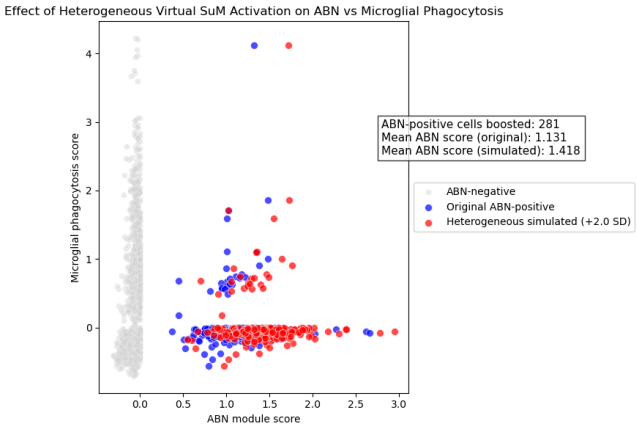

Figure 4. Heterogeneous virtual SuM activation of ABNs (+2 SD mean)

Heterogeneous virtual SuM activation of ABNs (+2 SD mean). Scatterplot depicts individual ABNs with normally distributed score perturbations (red), original ABN scores (blue), and ABN-negative cells (gray). Summary statistics are annotated to the right of the plot. Heterogeneous stimulation increases variability in ABN scores but does not generate consistent correlations with microglial phagocytosis.

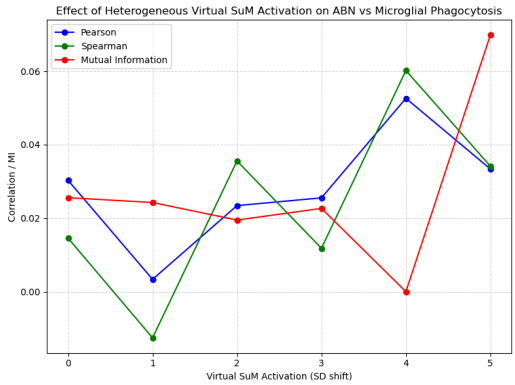

Figure 5. Iterative heterogeneous SD shift simulation (0–5 SD)

Iterative heterogeneous SD shift simulation (0–5 SD). Line plots show Pearson (blue), Spearman (green), and mutual information (red) for ABN-positive cells subjected to increasingly strong heterogeneous activation. Minor fluctuations in correlation metrics are observed, but no strong or consistent association emerges between ABN and microglial phagocytosis.

Table 3. Correlation metrics under heterogeneous SuM activation (progressive SD shifts, 0–5)

SD shift	Pearson	Spearman	Mutual Information
0	0.0303	0.0146	0.0256
1	0.0034	-0.0126	0.0243
2	0.0234	0.0356	0.0195
3	0.0255	0.0118	0.0227
4	0.0526	0.0602	0.0000
5	0.0334	0.0342	0.0698

DOI: 10.54254/2753-8818/2025.AU30835

Correlation metrics under heterogeneous virtual SuM activation. ABN-positive cells were subjected to normally distributed perturbations proportional to their SD, with shifts ranging from 0 to 5 SD. Minor fluctuations in correlation metrics indicate heterogeneous stimulation introduces variability without producing consistent strong associations.

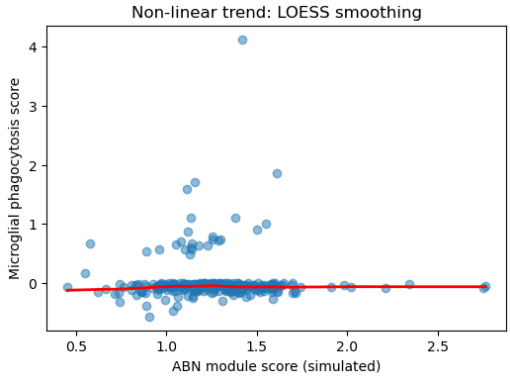

Figure 6. LOESS-smoothed trend of microglial phagocytosis against simulated ABN module scores

LOESS-smoothed trend of microglial phagocytosis against simulated ABN module scores. Non-linear regression shows a fitted red curve over the scatter of ABN-positive cells (red) after heterogeneous simulation. This visualization confirms the absence of strong non-linear relationships between ABN activation and microglial response.

Collectively, these analyses suggest that ABN activation, whether homogeneous or heterogeneous, increases module scores but does not produce strong or consistent correlations with TREM2+ microglial phagocytosis. These results underscore the importance of biological heterogeneity and indicate that additional mechanisms—such as local connectivity, secreted factors, or microenvironmental cues—may modulate microglial function.

5. Discussion

The findings highlight the critical role of heterogeneity in ABN–microglia interactions. Uniform ABN activation fails to alter correlations, indicating that biological variability and dynamic patterns of ABN activity are essential for modulating microglial states. Even with heterogeneous stimulation, the observed correlations remain modest, suggesting that direct coupling between ABNs and microglial phagocytosis is weak. These results imply that additional mechanisms, including neuronal connectivity, secreted signaling molecules, or the local microenvironment, contribute to microglial regulation.

From a methodological perspective, the computational framework provides a blueprint for stepwise hypothesis testing, offering a cost-effective approach to refine experimental designs. Future wet-lab studies should consider ABN heterogeneity, spatiotemporal dynamics, and network-level interactions when probing neuroimmune crosstalk. Incorporating these considerations may be critical to identify interventions capable of enhancing microglial plaque clearance in AD.

6. Conclusion

This computational modeling demonstrates that simple linear or homogeneous stimulation of ABNs is insufficient to drive TREM2+ microglial phagocytosis. Introducing dynamic, heterogeneous ABN activation better reflects potential biological variability but does not produce strong or consistent

DOI: 10.54254/2753-8818/2025.AU30835

correlations. This work provides a proof-of-concept computational pipeline for testing neurogenesis–microglia interactions, informing the design of future in vivo experiments.

References

[1] Ulland, T. K., & Colonna, M. (2018). TREM2—a key player in microglial biology and Alzheimer's disease. Nature Reviews Neurology, 14(11), 667–675. DOI: 10.1038/s41582-018-0072-1

[2] Lazarov, O., & Hollands, C. (2016). Hippocampal neurogenesis: Learning to remember. Progress in Neurobiology, 138–140, 1–18. https: //doi.org/10.1016/j.pneurobio.2015.12.006

[3] Li, Y.-D., Luo, Y.-J., Xie, L., Tart, D. S., Sheehy, R. N., Zhang, L., Coleman, L. G., Jr., Chen, X., & Song, J. (2023). Activation of hypothalamic-enhanced adult-born neurons restores cognitive and affective function in Alzheimer's disease. Cell Stem Cell, 30(4), 415–432.e6. https: //doi.org/10.1016/j.stem.2023.02.006

[4] Benesty, J., Chen, J., Huang, Y., & Cohen, I. (2009). Pearson correlation coefficient. In Noise reduction in speech processing (pp. 1–4). Springer.

[5] Spearman, C. (1904). The proof and measurement of association between two things. The American Journal of Psychology, 15(1), 72–101.

[6] McDavid, A., Finak, G., Chattopadyay, P. K., Dominguez, M., Lamoreaux, L., Ma, S. S., Roederer, M., & Gottardo, R. (2013). Data exploration, quality control and testing in single-cell qPCR-based gene expression experiments. Bioinformatics, 29(4), 461–467.

[7] Cover, T. M., & Thomas, J. A. (2006). Elements of information theory (2nd ed.). Wiley.

[8] Kraskov, A., Stögbauer, H., & Grassberger, P. (2004). Estimating mutual information. Physical Review E, 69(6), 066138.

[9] Chan, T. E., Stumpf, M. P. H., & Babtie, A. C. (2017). Gene regulatory network inference from single-cell data using multivariate information measures. Cell Systems, 5(3), 251–267.

[10] Cleveland, W. S. (1979). Robust locally weighted regression and smoothing scatterplots. Journal of the American Statistical Association, 74(368), 829–836.

[11] Trapnell, C., Cacchiarelli, D., Grimsby, J., Pokharel, P., Li, S., Morse, M., ... & Rinn, J. L. (2014). The dynamics and regulators of cell fate decisions are revealed by pseudotemporal ordering of single cells. Nature Biotechnology, 32(4), 381–386.

[12] Svensson, V., Vento-Tormo, R., & Teichmann, S. A. (2018). Exponential scaling of single-cell RNA-seq in the past decade. Nature Protocols, 13(4), 599–604.

[13] NCBI Gene Expression Omnibus (GEO). (n.d.). GSE140511. Supplementary file. (GSM4160643_WT_Cor_genes.tsv.gz; GSM4160643_WT_Cor_matrix.mtx.gz; GSM4160644_Trem2_KO_Cor_genes.tsv.gz; GSM4160644_Trem2_KO_Cor_matrix.mtx.gz; GSM4160645_WT_5XFAD_Cor_genes.tsv.gz; GSM4160645_WT_5XFAD_Cor_matrix.mtx.gz) https: //www.ncbi.nlm.nih.gov/geo/query/acc.cgi?acc=GSE140511)

[14] Yates, A. D., Allen, J., Amode, R. M., Azov, A. G., Barba, M., Becerra, A., Bhai, J., Campbell, L. I., Carbajo Martinez, M., Chakiachvili, M., Chougule, K., Christensen, M., Contreras-Moreira, B., Cuzick, A., Da Rin Fioretto, L., Davis, P., De Silva, N. H., Diamantakis, S., Dyer, S., Elser, J., Filippi, C. V., Gall, A., Grigoriadis, D., Guijarro-Clarke, C., Gupta, P., Hammond-Kosack, K. E., Howe, K. L., Jaiswal, P., Kaikala, V., Kumar, V., Langridge, N., Le, T., Luypaert, M., Maslen, G. L., Maurel, T., Moore, B., Muffato, M., Mushtaq, A., Naamati, G., Naithani, S., Olson, A., Parker, A., Paulini, M., Pedro, H., Perry, E., Preece, J., Quinton-Tulloch, M., Rodgers, F., Rosello, M., Ruffier, M., Seager, J., Sitnik, V., Szpak, M., Tate, J., Tello-Ruiz, M. K., Trevanion, S. J., Urban, M., Ware, D., Wei, S., Williams, G., Winterbottom, A., & Flicek, P. (2022). Ensembl Genomes 2022: an expanding genome resource for non-vertebrates. Nucleic Acids Research, 50(D1), D337–D343. https: //doi.org/10.1093/nar/gkab1064